Investigation on the fracture behavior of foamed concrete

Available online at www.sciencedirect.com

ScienceDirect

Procedia Structural Integrity 18 (2019) 525–531

Structural Integrity Procedia

www.elsevier.com/locate/procedia

25th International Conference on Fracture and Structural Integrity

Investigation on the fracture behavior of foamed concrete

Devid Falliano[a], Dario De Domenico[a]*, Antonino Sciarrone[a], Giuseppe Ricciardi[a], Luciana Restuccia[b], Giuseppe Ferro[b], Jean-Marc Tulliani[c], Ernesto Gugliandolo[d]

[a] *Department of Engineering, University of Messina, Contrada Di Dio, 98166 Sant'Agata, Messina, Italy*
[b] *Department of Structural, Geotechnical and Building Engineering, Politecnico di Torino, Corso Duca degli Abruzzi, 24, 10129 Turin, Italy*
[c] *Department of Applied Science and Technology, Politecnico di Torino, Corso Duca degli Abruzzi, 24, 10129, Turin, Italy*
[d] *G. Gugliandolo Srl, Via Galileo Galilei 8, 98124, Messina, Italy*

Abstract

The fracture behavior of lightweight foamed concrete (LWFC) is significantly influenced by microstructural properties, which are ascribed to the arrangement of air bubbles and pores as well as to the presence of different hydration products. In this contribution, an experimental investigation on the fracture behavior of LWFC is performed. Notched beams made of LWFC were tested in three-point bending to determine the fracture energy based on the load-CMOD (Crack Mouth Opening Displacement) curve. The influence of the dry density is explored considering one density for non-structural purposes (equal to 800 kg/m^3) and another density for structural applications (1600 kg/m^3). Moreover, two curing conditions are considered (air and water). The load-CMOD curves reveal that for lower dry densities the fracture behavior of LWFC is particularly affected by the curing conditions, with better results achieved in air curing conditions, but this influence decreases with higher dry densities. The improved performance in air curing conditions for lower dry densities is also observed in terms of flexural strength, but is not particularly evident for the compressive strength. Micrographs across the crack surface determined via Scanning Electron Microscopy (SEM) are finally presented to analyze the experimental findings and justify the results in terms of microstructural configuration of the specimens.

Peer-review under responsibility of the Gruppo Italiano Frattura (IGF) ExCo.

Keywords: foamed concrete; curing conditions; dry density; lightweight concrete; fracture energy; flexural strength.

* Corresponding author. Tel.: +39-0906765921
E-mail address: dario.dedomenico@unime.it

2452-3216
Peer-review under responsibility of the Gruppo Italiano Frattura (IGF) ExCo.
10.1016/j.prostr.2019.08.196

1. Introduction

Foamed concrete, obtained through addition of preformed foam into the cement paste, is an attractive construction material because of its lightweight properties associated with thermal insulation, acoustic absorption and fire resistance, especially in the low-density range [Wei et al. 2013; Falliano et al. 2019c; Kim et al. 2012; Valore 1954]. Moreover, previous studies demonstrated that the mechanical performances of foamed concrete can be improved by the introduction of mineral additions, like fly ash and silica fume [Jones and McCarthy 2005], or through the use of fibers of different nature [Falliano et al. 2019a; Ramamurthy et al. 2009; Bing et al., 2011; Kayali et al. 2003] or bi-directional grid reinforcement [Falliano et al. 2019b]. It has been found that the mechanical properties of foamed concrete depend on the dry density, curing condition, foaming agent, and cement type [Falliano et al. 2018a; 2018b; Panesar 2013].

This study aims to expand the knowledge of the fracture behavior of lightweight foamed concrete (LWFC), because, to the authors' best knowledge, relatively few research studies are present in the relevant literature [Kozłowski et al. 2015; Kozłowski and Kadela 2018]. Previous studies showed that the fracture energy of foamed concrete is lower than that of ordinary concrete, generally < 25N/m [Hengst and Tressler, 1983]. In this experimental campaign, a new type of foamed concrete is analyzed, which is prepared with a specific viscosity enhancing agent (VEA) that increases consistency and viscosity at the fresh state. This VEA not only allows the production of foamed concrete via an extrusion process, but also makes this material suitable for 3D printing applications – the resulting material is called "extrudable lightweight foamed concrete" (ELWFC).

A series of 24 notched beams made of ELWFC are prepared: 16 reached a final dry density of 800 kg/m^3 (for non-structural purposes, in order to exploit the acoustic absorption and thermal insulation properties) and 8 reached a final dry density of 1600 kg/m^3 (more appropriate for structural applications with a lower self-weight in comparison with ordinary concrete elements). The specimens prepared with such two dry densities are then cured in two different conditions, namely in air at environmental temperature of 20°C and in water at controlled temperature of 20°C. In this manner, the influence of dry density and curing condition on the resulting fracture behavior of ELWFC is analyzed. In particular, prismatic notched specimens are prepared and tested according to JCI-S-001 standards, namely three-point bending tests in CMOD (Crack Mouth Opening Displacement) mode, in order to evaluate the fracture energy G_F. Comparison between specimens having different dry densities and curing conditions has been performed in terms of flexural and compressive strength values, as well as load-CMOD curves, fracture energy, and related ductility. At the end of the mechanical experimental campaign, some specimens were also analyzed through Scanning Electron Microscopy (SEM) in order to further justify the fracture behavior, based on the microstructural configuration of the specimens.

2. Preparation of the specimens and testing conditions

The notched beams of ELWFC were tested according to JCI-S-001 standards [JCI-S-001, 2003]. The dimensions of the beams are 20x20x80mm^3 and the tests were carried out in displacement controlled mode using a Zwick Line-Z010 testing equipment [Ahmad et al., 2015; Restuccia and Ferro, 2016; Restuccia et al. 2017; Restuccia and Ferro, 2018] having a 1 kN load capacity. A Portland CEM I 52.5 R was used with a water-to-cement ratio equal to 0.3 and VEA was added to the cement mix to increase the cohesion and viscosity at the fresh state, without altering the workability of the paste. The lightweight properties of the ELFWC is obtained through the addition of preformed foam, using a foam-to-cement ratio (in weight) equal to 0.3 for the 800kg/m^3 and equal to 0.08 for the 1600 kg/m^3 dry density. Such preformed foam was obtained through an appropriate foam generator, using a protein-based foaming agent (concentration of 5%) and the resulting foam density was nearly equal to 85g/L. More details on samples preparation are reported in [Falliano et al. 2018a].

The cement mixes are then poured in formworks and, afterwards, a half of specimens (12) were cured in air and the other half (12) in water. The fresh density of the two mixes (target dry density of 800 ± 50 kg/m^3 and 1600 ± 50 kg/m^3) was of 1041 kg/m^3 and of 1700 kg/m^3, respectively. After the tests, the specimens were dried in oven (at 110°C) until achievement of a constant weight in order to determine the actual dry density of the samples. After 28 days, the specimens were prepared for the mechanical tests and notched with a band saw in compliance with the JCI-S-001-2003 standards [JCI-S-001, 2003], as reported in Figure 1. In particular, the height of the notch ranged from 6.0

to 7.0 mm. To measure the CMOD, a clip-on strain gauge was installed at the two edges of the notch as illustrated in Figure 2.

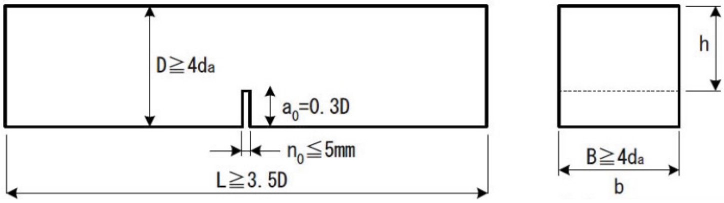

Figure 1 Dimensional requirements prescribed by JCI-S-001-2003 standards.

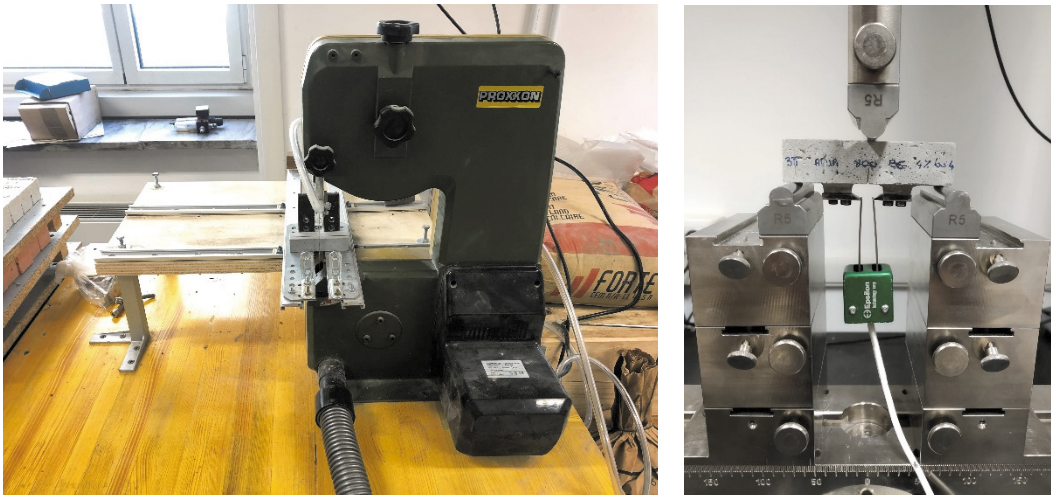

Figure 2 Preparation of the notch on the beams (left) and installation of clip-on strain gauge on the two edges (right).

The load was applied with a displacement rate of 0.005 mm/min, and the rollers are adjusted such that the resulting beam span was equal to 70 mm. After the beam collapsed, the two halves of the broken specimen were tested in compression in another testing equipment with load capacity of 50 kN and displacement rate of 0.5 mm/min.

3. Results and discussion

The main results of the experimental campaign are summarized in this section. The flexural strength σ_f of the samples is computed through the formula:

$$\sigma_f = \frac{3}{2}\frac{F_{\max}L}{bh^2} \text{ [MPa]} \tag{1}$$

where $F_{\max}$ denotes the maximum load [N], L is the span length [mm], b the specimen depth [mm] and h the net ligament height [mm] as shown in Figure 1. Moreover, the fracture energy G_F of the specimens is calculated through the expression reported in JCI-S-001 standards:

$$G_F = \frac{0.75W_0 + W_1}{A_{lig}} \text{ [N/m]} \tag{2}$$

where A_{lig} denotes the area of nominal ligament [mm^2], W_0 represents the area below the CMOD curve up to rupture of specimen [N·mm] and W_1 is the work done by the self-weight and the applied loading [N·mm], which is calculated as follows

$$W_1 = 0.75\left(\frac{\ell}{L}m_1 g + 2m_2 g\right)\mathrm{CMOD}_c \quad (3)$$

where L is the entire length of the specimen [mm], m_1 is the mass of the notched specimen [kg], m_2 represents the mass of the loading arrangement part not attached to the testing machine but placed on beam until rupture [mm], g is the acceleration of gravity [9.807 m/s^2] and CMOD_c is the crack mouth opening displacement at the rupture [mm].

The average results for the different classes of specimens are listed in Table 1. It is possible to notice that the curing conditions significantly affect the results in terms of flexural strength and fracture energy for the lower dry density of 800 kg/m^3, and the better performance is surprisingly observed in air curing conditions. However, this influence of the curing conditions becomes marginal in terms of compressive strength (with moderately higher values for air curing conditions). On the other hand, with increasing values of the dry density, the behavior becomes closer to that of ordinary (normal-weight) concretes. Consequently, this marked difference in terms of curing conditions is no longer apparent, and the results are more or less comparable in the two conditions. At the dry density value of 1600 kg/m^3 the compressive strength is higher than 40 MPa, which justifies the potential use of this material for structural applications.

Table 1. Average results of ELWFC specimens with different curing conditions and dry densities

Specimen class	CMOD at peak load	Flexural strength	Fracture energy	Compressive strength
	d_{Fmax} [mm]	σ_f [MPa]	G_F [N/m]	σ_c [MPa]
800 kg/m^3 air	0.0165	1.02	10.46	8.24
800 kg/m^3 water	0.0053	0.43	3.09	7.35
1600 kg/m^3 air	0.0167	3.28	21.80	46.15
1600 kg/m^3 water	0.0177	2.40	27.65	44.01

A set of comparative histograms of the results for different dry densities and curing conditions are shown in Figure 3. In these graphs, we can notice that passing from 800 to 1600 kg/m^3 there is an increase of flexural strength of almost 75%, an increase of the fracture energy of around 50% in air curing conditions, and an increase of the compressive strength of more than 80%. These increases are even more marked in water curing conditions, which is consistent with the previous remarks.

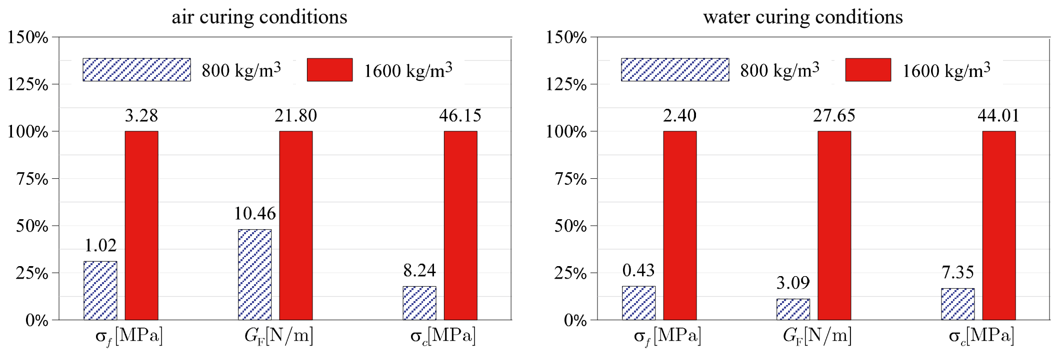

Figure 3. Comparative histograms of average flexural strength, fracture energy and compressive strength of LWFC cured in air and in water for two different dry densities of the specimens.

The load-CMOD curves are depicted in Figure 4 for two representative specimens, for the two different dry densities and curing conditions analyzed. In air (left-hand of the figure) the behavior is qualitatively similar, despite the lower level of load (and resulting flexural strength) for the lower dry density. Instead, in water there is a marked increase in the fracture energy (and the resulting area enclosed by the curve) for the higher dry density. Moreover, there is a significant increase of the ultimate displacement, which denotes an increase of ductility of the samples. There is a change of behavior for the two dry densities: the ultimate displacement in water for 1600 kg/m^3 is higher than that in air at the same dry density, whereas the ultimate displacement in water at 800 kg/m^3 is lower than that in air at the same dry density. The post-peak branch of the load-CMOD curve is more evident for higher densities, especially in water curing conditions.

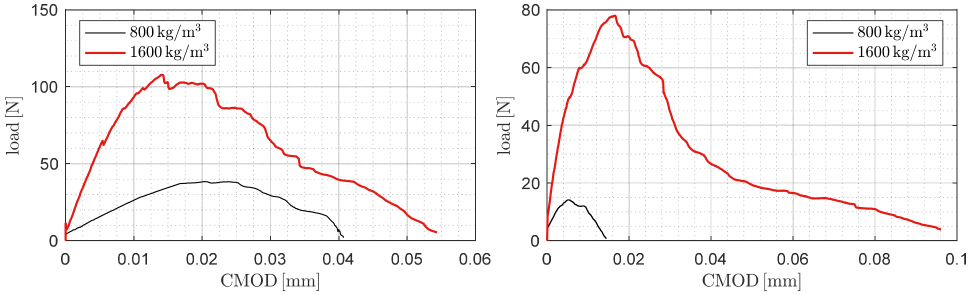

Figure 4. Comparison of load-CMOD curves from the three-point-bending test on two pairs of LWFC beams cured in air and in water.

The different fracture behavior observed in the specimens was further evaluated through SEM observations. In particular, in Figure 5 a qualitative comparison of the pores dimensions and distributions is shown for the two dry densities of 800 and 1600 kg/m^3. It is possible to appreciate that by increasing the dry density, the dimensions of the pores decrease and become more uniformly distributed throughout the cement matrix. This contributes to a higher mechanical performance in both flexure and compressive tests.

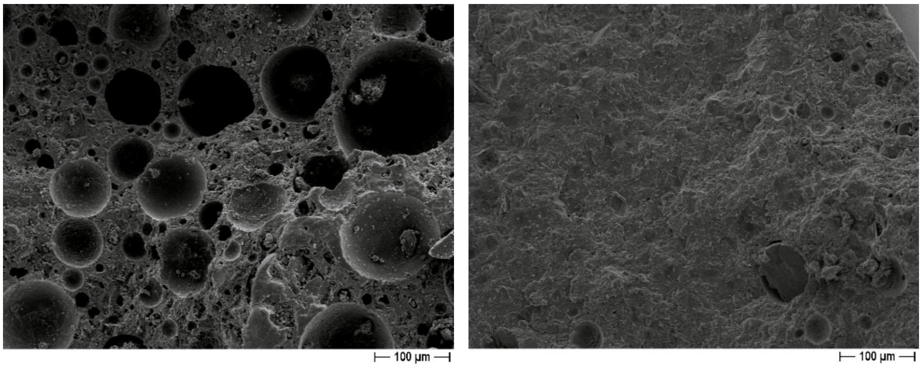

Figure 5. Qualitative comparison of pores dimensions and distribution through SEM micrographs of a representative portion of water-cured ELWFC specimen with a dry density of 800kg/m^3 (left) and 1600 kg/m^3 (right).

The SEM micrographs have given justifications on the different fracture behavior of air- and water-cured specimens for the lower dry density. In particular, specimens cured in air at 800 kg/m^3 have a more tortuous crack surface than specimens cured in water at the same dry density, which is responsible for the increase of the fracture energy reported in Table 1 and in the comparative histograms of Figure 3. Moreover, we also noticed that different curing conditions led to different morphology of the hydration products, especially close to the pores surface, where there is a high concentration of foaming agent molecules.

Two SEM micrographs of a representative portion of air-cured ELWFC specimen having density of 800 kg/m^3 extracted across the crack surface are reported in Figure 6. In this figure, the coalescence phenomena of the pores can be observed. This is particularly evident for lower dry densities, where these defects represent weak zones in the sample. Wider cracks and a more apparent crack pattern are observed in such class of specimens. The distribution of the pores is an important factor for the crack onset and development and, consequently, the final fracture energy value of the sample.

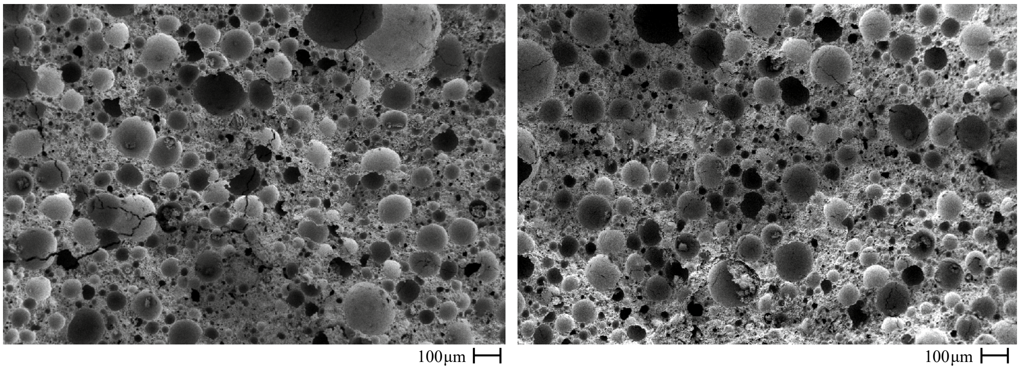

Figure 6. SEM micrographs of a representative portion of air-cured ELWFC specimens with 800 kg/m^3 along the crack surface representing how the crack pattern develops along the porosities in two different situations.

4. Conclusions

A series of tests on lightweight foamed cement paste notched beams were carried out. The fracture behavior was analyzed in terms of load-CMOD curve, in compliance with the JCI-S-001-2003 standards. These tests were performed to investigate the influence of the dry density and of the curing conditions on the resulting fracture energy, flexural strength and compressive strength of the specimens.

Based on the results of this experimental campaign, the following conclusions can be drawn:

1) The curing conditions play a more crucial role for the lower dry densities, and specimens cured in air exhibited better performance (in terms of both fracture energy and flexural strength) than specimens cured in water;
2) The curing conditions do not significantly affect the compressive strength values at the lower dry densities, although a better performance is achieved for air curing conditions;
3) The increase of the dry density obviously leads to an increase of the mechanical properties, which results in an increase of the load-CMOD curve and an increase of the fracture energy of around 50% for air curing conditions, and of more than 80% for water curing conditions;
4) The microstructural tortuosity of the specimens, ascribed to the distribution and dimensions of the pores as well as to the different morphology of the hydration products (not discussed in this paper), explains the different macroscopic behavior observed in the tests;
5) The compressive strength of specimens with 1600 kg/m^3 is around 45 MPa, which allows the potential use of this material for structural applications, benefitting from the advantages related to the lower self-weight.

References

Ahmad, S., Tulliani, J.M., Ferro, G.A., Khushnood, R.A., Restuccia, L., Jagdale, P., 2015. Crack path & fracture surface modifications in enhanced cement composites. Frattura ed Integrità Strutturale; 34: 524-533.

Bing, C., Zhen, W., Ning, L., 2011. Experimental research on properties of high-strength foamed concrete. Journal of Materials in Civil Engineering; 24(1):113-118.

Falliano, D., De Domenico, D., Ricciardi, G., Gugliandolo, E., 2019a. Compressive and flexural strength of fiber-reinforced foamed concrete: Effect of fiber content, curing conditions and dry density. Construction and Building Materials; 198: 479-493.

Falliano, D., De Domenico, D., Ricciardi, G., Gugliandolo, E., 2018a, Experimental investigation on the compressive strength of foamed concrete: Effect of curing conditions, cement type, foaming agent and dry density. Construction and Building Materials; 165: 735-749.

Falliano, D., De Domenico, D., Ricciardi, G., Gugliandolo, E., 2019b. Improving the flexural capacity of extrudable foamed concrete with glass-fiber bi-directional grid reinforcement: An experimental study. Composite Structures; 209: 45-59.

Falliano, D., De Domenico, D., Ricciardi, G., Gugliandolo, E., 2018b. Key factors affecting the compressive strength of foamed concrete. In IOP Conference Series: Materials Science and Engineering; 431(6), p. 062009, IOP Publishing.

Falliano, D., Gugliandolo, E., De Domenico, D., Ricciardi, G., 2019c. Experimental Investigation on the Mechanical Strength and Thermal Conductivity of Extrudable Foamed Concrete and Preliminary Views on Its Potential Application in 3D Printed Multilayer Insulating Panels. In: First RILEM International Conference on Concrete and Digital Fabrication – Digital Concrete 2018, Springer, Cham, pp. 277-286, DOI: 10.1007/978-3-319-99519-9_26.

Hengst, R.R., Tressler, R.E., 1983. Fracture of foamed Portland cements. Cement and Concrete Research; 13(1): 127-134.

JCI-S-001, 2003. Method of Test for Fracture Energy of Concrete by use of Notched Beam, Japan Concrete Institute, Tokyo, Japan.

Jones, M.R., McCarthy, A., 2005. Preliminary views on the potential of foamed concrete as a structural material. Magazine of concrete research; 57(1): 21-31.

Kayali, O., Haque, M.N., Zhu, B., 2003. Some characteristics of high strength fiber reinforced lightweight aggregate concrete. Cement and Concrete Composites; 25(2): 207-213.

Kim, H.K., Jeon, J.H., Lee, H.K., 2012. Workability, and mechanical, acoustic and thermal properties of lightweight aggregate concrete with a high volume of entrained air. Construction and Building Materials; 29: 193-200.

Kozłowski, M., Kadela, M., Kukiełka, A., 2015. Fracture energy of foamed concrete based on three-point bending test on notched beams. Procedia Engineering; 108: 349-354.

Kozłowski, M., Kadela, M., 2018. Combined Experimental and Numerical Study on Fracture Behaviour of Low–Density Foamed Concrete. In IOP Conference Series: Materials Science and Engineering; 324(1), p. 012031. IOP Publishing.

Panesar, D.K.. 2013. Cellular concrete properties and the effect of synthetic and protein foaming agents. Construction and Building Materials; 44: 575-584.

Ramamurthy, K., Nambiar, E.K., Ranjani, G.I.S., 2009. A classification of studies on properties of foam concrete. Cement and Concrete Composites; 31(6): 388-396.

Restuccia, L., Ferro, G.A., 2016. Promising low cost carbon-based materials to improve strength and toughness in cement composites. Constr. Build. Mater.; 126: 1034-1043.

Restuccia, L., Reggio, A., Ferro, G.A., Kamranirad, R., 2017. Fractal analysis of crack paths into innovative carbon-based cementitious composites. Theoretical and Applied Fracture Mechanics; 90: 133-141.

Restuccia, L., Ferro, G.A., 2018. Influence of filler size on the mechanical properties of cement-based composites. Fatigue and Fracture of Engineering Materials and Structures; 41(4): 797-805.

Valore, R.C., 1954. Cellular concrete part 2 physical properties. ACI J; 50:817–36.

Wei, S., Yiqiang, C., Yunsheng, Z., Jones, M.R., 2013. Characterization and simulation of microstructure and thermal properties of foamed concrete. Construction and Building Materials; 47: 1278-1291.